European Review for Medical and Pharmacological Sciences 2023; 27: 5338-5355

Exploration of the influence of early rehabilitation training on circulating endothelial progenitor cell mobilization in patients with acute ischemic stroke and its related mechanism under a lightweight artificial intelligence algorithm

L. SUN[1], H. ZHANG[2], Y.-M. YANG[1], X.-S. WANG[1]

[1]Department of Internal Medicine, People's Hospital of Yanshan County, Cangzhou, Hebei, China
[2]Department of Emergency Nursing, Yanshan Fude Hospital, Cangzhou, Hebei, China

Abstract. – OBJECTIVE: This work aimed to explore the application of lightweight artificial intelligence algorithms in magnetic resonance imaging (MRI) image processing of patients with acute ischemic stroke (AIS) to clarify the effect and mechanism of early rehabilitation training on the mobilization of circulating endothelial progenitor cells (EPCs) in AIS.

PATIENTS AND METHODS: A total of 98 AIS patients undergoing MRI examination were selected as the research objects and were randomly divided into a rehabilitation group (early rehabilitation training, 50 cases) and a routine group (conventional treatment, 48 cases) by random number table method and lottery method. In this work, based on the convolutional neural network (CNN) algorithm, a low-rank decomposition algorithm was introduced to optimize it, and a lightweight MRI image computer intelligent segmentation model (LT-RCNN) was established. The LT-RCNN model was used in the MRI image processing of AIS patients, and the role of the model in AIS image segmentation and lesion localization was analyzed. Furthermore, flow cytometry was used to detect the number of peripheral circulating EPCs and CD34+KDR+ cells in the two groups of patients before and after treatment. The serum levels of vascular endothelial growth factor (VEGF), tumor necrosis factor-α (TNF-α), interleukin 10 (IL-10), and stromal cell-derived factor-1α (SDF-1α) content were detected by Enzyme-Linked Immunosorbent Assay (ELISA). In addition, the correlation between each factor and CD34+KDR+ was analyzed by Pearson linear correlation.

RESULTS: The diffusion-weighted imaging (DWI) signal of MRI images of AIS patients under the LT-RCNN model was high. The location of the lesion could be accurately detected, and the contour of the lesion could be displayed and segmented, and the segmentation accuracy and sensitivity were significantly better than before optimization. The number of EPCs and CD34+KDR+ cells in the rehabilitation group was increased compared with the control group ($p<0.01$); the expression levels of VEGF, IL-10, and SDF-1α were higher than those of the control group ($p<0.001$), and TNF-α content was lower than the control group ($p<0.001$). The number of CD34+KDR+ cells was positively correlated with VEGF, IL-10, and TNF-α contents ($p<0.01$).

CONCLUSIONS: The results showed that the computer-intelligent segmentation model LT-RCNN could accurately locate, and segment AIS lesions and the early rehabilitation training could change the expression level of inflammatory factors and further promote the mobilization of AIS circulation EPCs.

Key Words:
Magnetic resonance imaging, Acute ischemic stroke endothelial progenitor cells, Lightweight artificial intelligence, Algorithm segmentation.

Introduction

Stroke is a neurological disease with high disability and is one of the major causes of death worldwide[1]. According to the relevant investigation conducted by World Health Organization (WHO), the incidence of stroke in China is the highest around the world. In China, about 1.5 million people suffer from stroke every year. The proportion of new patients with stroke reaches 109.7 to 217/100,000 people[2] and patients with ischemic stroke account for around 85% among all patients with stroke with mortality over 20%[3]. According to the duration after the occurrence of ischemic stroke, the lesion phases are divided into acute phase, subacute phase, and chronic phase. Acute ischemic stroke (AIS) is pathologically

Corresponding Author: Lei Sun, MD; e-mail: 19931729535@163.com

based on cerebral vascular arteriosclerosis and is featured with high morbidity, disability, and relapse. At present, the main clinical methods for observing lesions among stroke patients include computed tomography (CT) and magnetic resonance imaging (MRI). MRI is sensitive to ischemic neurons and can express the tissue usability of water molecules more effectively to improve the detection rate of early lesions[4]. As artificial intelligence technology develops, manual delineations of lesion areas are gradually replaced with a deep learning algorithm because of objectivity, repeatability, and scalability. However, a convolutional neural network (CNN) contains a large number of parameters in the processing of large batch of medical images. As a result, the computing cost and operational capability of the graphics processing unit were increased, which limits its wide application in processing medical images[5]. Hence, some scholars propose to establish a lightweight deep learning network by improving the hardware performance or compressing the network algorithmically to reduce storage and computing costs[6]. However, there are few researches in literature on lightweight deep learning model in medical image processing.

At present, thrombolysis is the main clinical treatment method for AIS. However, the time window for thrombolysis was short among AIS patients, thus most patients could not get to the hospitals where thrombolysis could be implemented within the period. Consequently, the complications' incidence among AIS patients increased[7]. Limb motor dysfunction is a common complication of AIS. The best period for rehabilitation is within 1 month after stroke and early rehabilitation is defined as the recovery within 3 months[8]. Scientific and effective rehabilitation training plays a positive role in establishing brain collateral circulation and restoring neurological function and limb motor ability. At present, rehabilitation training has been performed on the posterior limbs of stroke patients by some researchers[9,10]. It was demonstrated that the method could help restore the motor functions of lower limbs among stroke patients while having no remarkable efficacy in upper limb rehabilitation. As a result, overall rehabilitation progression was delayed[11]. In addition, it was demonstrated in some research[12] that a rehabilitation training intervention for patients with stroke could effectively improve brain and limb function of patients and mobilize stem cells.

Abnormal vascular endothelial function is positively correlated with AIS[13]. Endothelial progenitor cells (EPCs) play a vital role in the proliferation and differentiation of endothelial cells, such as maintaining the integrity of the vascular endothelium, repairing impaired blood vessels, and promoting vascular regeneration[14]. Normally, the expression of peripheral circulatory EPCs remains stable. When tissues are impaired (infection, stroke, and myocardial infarction), the expression of peripheral circulatory EPCs will notably rise and get involved in brain tissue modification, neoangiogenesis, wound healing, ischemia injury, tumor growth, and other physiological and pathological processes[15]. It is shown that the expression of EPCs gradually increases within 7 days after AIS occurs[16]. EPCs can differentiate into mature endothelial cells to get involved in vascular regeneration to promote the recovery of ischemia events[17]. Zhao et al[18] concluded that EPCs showed significant therapeutic effects on animals with cardiac ischemia. CD34 + cells originating from bone marrow contained EPCs and hematopoietic stem cells, which were involved in the angiogenesis of impaired tissues to improve the myocardial function of ischemic heart disease.

To sum up, compared with other application fields, lightweight deep learning model in medical image processing is still at a relatively preliminary stage[19,20]. EPCs played a vital role in the occurrence and development of stroke. Although early rehabilitation training could improve brain and limb function of patients with stroke, its influence on EPCs and the specific mechanism on the recovery of brain and limb functions of patients were still unknown. Hence, CNN algorithm was optimized to establish a lightweight CNN learning model, which was applied in the processing of diagnostic MRI images among AIS patients. The potential application values of the learning model were analyzed. At the same time, early rehabilitation training was used to intervene in AIS patients, and the influence of early rehabilitation training on circulation EPCs mobilization in AIS patients was discussed. Moreover, the specific mechanism of early rehabilitation training on the recovery of brain and limb functions of AIS patients was analyzed to provide some theoretical basis for the treatment and nursing of AIS patients.

Patients and Methods

Research Objects and Grouping

98 AIS patients treated in People's Hospital of Yanshan County between October 2020 and December 2021 were selected, including

57 males (58.16%) and 41 females (41.84%). They were aged between 51 and 87 with an average of 66.31±9.47.

The inclusion criteria were as follows:

A. Patients who met the diagnostic standards for AIS[21] and were diagnosed with AIS by cranial magnetic resonance imaging examination.
B. Patients were admitted to the hospital within 24 hours after the incidence of AIS.
C. Patients with National Institute of Health stroke scale (NIHSS) scores between 8 and 24 points.
D. Patients suffering from AIS for the first time.
E. Patients aged over 50.
F. Patients who were able to respond to verbal instructions.

The exclusion criteria were as follows:

A. Patients with intracranial hemorrhage or tumor.
B. Patients with acute and chronic inflammatory diseases.
C. Patients with severe complicated heart, liver, kidney, and other visceral dysfunctions.
D. Patients undergoing thrombolytic treatment.
E. Patients with complicated coma, audiovisual disorders, and progressive stroke.
F. Patients with exacerbated disease, such as new infarction or hemorrhage.
G. Patients receiving craniocerebral surgery within the past 3 months.
H. Patients with blood system diseases.
I. Patients with chronic heart failure.

The experimental procedures had been approved by the Hospital Ethics Committee of People's Hospital of Yanshan County. All included research objects had signed informed consent forms.

98 AIS patients were randomly enrolled into the rehabilitation group (50 cases undergoing early rehabilitation training based on routine therapy for AIS) and conventional group (48 cases performed with conventional therapy) by random number table method and lottery method.

MRI Scan Method

Toshiba Atlas 1.5T superconducting MRI system (Tokyo, Japan) and head matrix coil were adopted to perform routine MRI (T1 weighted imaging, T2 weighted imaging, and diffusion-weighted imaging) and routine horizontal axial imaging and coronal plane imaging. The scan parameters of T1 weighted imaging were set as follows. The time of repetition was 540 ms and the time of echo was 11 ms. The scan parameters of T2 weighted imaging were set as follows; the time of repetition was 4,000 ms and the time of echo was 97 ms. The scan parameters of diffusion-weighted imaging were set as follows; time of repetition was 2,900 ms, the time of echo was 89 ms, b-0, and 1,000 s/mm^2. The field of view was 207×207 mm, the matrix size was 64×64, the number of slices was 9, and the slice thickness was 8 mm.

Lightweight CNN Model-Based MRI Processing Method

Singular value decomposition and low-rank decomposition in matrix decomposition are the commonly used compression acceleration algorithms of lightweight models. In CNN, convolutional mainly affects the computation amount of the network, while the fully connected layer affects the size of the network model store. To solve the problems in CNN, the matrix two-dimensional singular value decomposition (SVD) algorithm could be extended to a three-dimensional convolution kernel[22]. A singular value decomposition algorithm was employed to decompose the original matrix into the product of the upper triangular matrix, diagonal matrix, and lower triangular matrix. After that, only the most important eigenvalues in the diagonal matrix were taken to reduce the number of parameters, model size, and the duration of forward propagation. It is assumed that the data for input layer is A with a size of $\alpha \times \beta$. Besides, the weight matrix is represented by W. The output data in the connected layer were expressed as follows in equation (1).

$$Y=Wa \tag{1}$$

After the decomposition, the approximate value of W was expressed as follows in equation (2).

$$W=B\sum C^T \approx B\sum_t C^T \tag{2}$$

In equation (2), B refers to the orthogonal matrix of a α×t dimension. $\sum_t C^T$ represented the diagonal matrix of the first t^{th} values in the corresponding original diagonal matrix W and its dimension was t ×t. C denoted the diagonal matrix of a $\beta \times t$ dimension.

The calculation method for singular value decomposition was as follows in equation (3).

$$Y=Wa \approx B\sum_t C^T a \tag{3}$$

Model compression by singular value decomposition resulted in the loss of accuracy. Based

on singular value decomposition, low-rank decomposition was introduced to effectively eliminate the convolution kernel redundancy. It was assumed that the convolution kernel in the CNN algorithm was 4D tensor $W \in R^{N \times d \times d \times E}$. N and E represent the number of output and input feature maps and d refers to the size of the convolution kernel. The feature map of the output image was expressed as follows in equation (4).

$$F_n(x,y)=\sum_{(n=1)}^{E}\sum_{(x'=1)}^{X}\sum_{(y'=1)}^{Y}Z^c(x^l,y^l)W_n^E(x\text{-}x^l,y\text{-}y^l) \quad (4)$$

In equation (4), W_n^e referred to the c^{th} channel of the n^{th} filter. Besides, X and Y denote the width and height of feature maps, respectively. Minimized objective function was expressed in equation (5) as follows.

$$G_1(H,V)=\sum_{n,E}\|W_n^E-\sum_{(k=1)}^{K}H_n^k(V_k^E)^T\|_F^2 \quad (5)$$

In equation (5), H and V are referred to the horizontal and vertical filters, respectively. In addition, K and T denote the hyperparameter of the controlled rank and tensor mapping matrix, respectively. Based on the matrix decomposition lightweight model, network depth was adopted to replace the network width. A small convolution kernel and a global average pooling layer were used to replace the full connected layer to establish LT-RCNN. The specific calculation process of the algorithm was as follows. Firstly, the input MRI images were calculated by CNN algorithm. Then, the features of MRI images were extracted, and the region proposal network slid on the feature map to generate the corresponding feature vectors. After that, they were input into the convolution layer and the parameters in the fully connected layer were modified. Finally, the Softmax layer was used to convert the output scores into a confidence level of whether the targets to be tested were contained. Candidate regions were preliminarily obtained, and their mechanical energies were classified and accurately localized. Consequently, the segmentation results of MRI lesions were acquired.

Treatment Methods for AIS Patients

AIS patients in both conventional and rehabilitation groups were treated with routine therapy, including drug therapy, physical factor therapy, and basic rehabilitation training. Based on routine therapy and intervention, AIS patients in the rehabilitation group performed early rehabilitation training immediately after the disease became stable. The specific contents of the rehabilitation training were as follows.

A. Sitting position and decubitus training; B. ability to balance in a sitting position; C. ability to balance in a standing position; D. gait; E. ability to interchange sitting and standing positions; F. daily living activities; G. good limb placement at the interval training; H. application of orthosis; I. activities of daily living training; L. cognitive ability (the training item was implemented according to the severity of disorders, such as reading a newspaper and ordering numbers); M. social adaption ability (mainly at the psychological level), including giving a comprehensive and detailed introduction of the patient's condition to the family members, and obtaining their recognition and understanding. This could help the family to understand the patient's situation and fully support and encourage the patient during the recovery process. By establishing a support system and a positive attitude, patients could address concerns, cooperate with treatment and recover as quickly as possible. This could help patients to integrate smoothly into the society and ensure them a good quality of life.

In the control group, the vital signs of stroke remained stable for 7 days before rehabilitation training.

At the neurology department, a rehabilitation scheme was formulated for the patients in two groups by therapists according to the patient's actual conditions. Patients were guided to carry out rehabilitation training with the cooperation of their family members. Patients who met discharge indications, such as those with restored limb function or those with mild limb dysfunction who were required to perform home rehabilitation, could carry out home rehabilitation training under the guidance of therapists. They should visit the rehabilitation department for reexamination regularly. The rest of the patients were transferred to the rehabilitation department for further rehabilitation treatment. After the grouping, all scale statistics were conducted in hospitals. Each item of the scale was observed, assessed, and scored by professionals on-site to ensure the effectiveness and objectivity of data.

The above was performed once per day and lasted for 45 mins to 60 mins. The patients performed the rehabilitation training for 2 consecutive weeks. During hospitalization, patients and their family members were urged to master the training methods. After discharge, their family members needed to supervise and guide patients.

Evaluation of Therapeutic Effects

The clinical and therapeutic effects on patients in the two groups before and after intervention were assessed. Firstly, Fugl-Meyer assessment (FMA) scale[23] was employed to evaluate motor function. The total score was 100 points, including 66 points for the upper limbs and 34 points for the lower limbs. FMA score was positively correlated with motor function. Modified Barthel index (MBI)[24] was utilized to assess the activity of daily living. MBI score ≥60, MBI score between 41 and 59, and MBI score ≤40 represented mild, moderate, and severe dysfunction, respectively. The National Institutes of Health Stroke Scale (NIHSS) was adopted to evaluate the severity of neurological dysfunction. The total score of NIHSS scale[25] was 42 points. A higher score indicated severer neurological dysfunction. Stroke-specific quality of life (SS-QOL)26 was utilized to evaluate quality of life. The total score amounted to 245 points. The score was positively correlated with quality of life.

Detection of the Number of Peripheral Circulatory EPCs and CD34+ Kinase Insertion Domain Receptor (KDR) + Cells by Flow Cytometry

5 mL venous blood of AIS patients was extracted and placed into anticoagulation tubes 1 d, 8 d, and 15 d after the intervention. After that, it was used for the detection of the number of EPCs and CD34+KDR+ cells. Elite flow cytometry (Coulter Company, Florida, US) was used to detect the above two indicators. The specific detection method for peripheral circulatory EPCs was as follows. Firstly, 50 μL antithrombin was added to 20 μL fluorescein isothiocyanate (FITC)-labeled CD34 monoclonal antibody IgG1 (Biolegend, Inc, CA, USA) and 20 μL phosphatidylethanolamine (PE)-labeled kinase insertion domain receptor (KDR) monoclonal antibody (Biolegend, Inc.). After that, the mixed solution was placed away from the light at room temperature for 30 mins. Next, it was added to red blood cell lysis buffer and then placed for 10 mins (Beijing Bioss Biotechnology Co., Ltd.). Then, it was centrifuged at 1,000 rpm/min for 5 mins. After centrifugation, the precipitates were collected, and the mixture was rinsed with phosphate buffer saline (PBS). Under two-way scattered light, the number and percentage of CD34+KDR+ cells were detected. The percentage was recorded as the expression of peripheral circulatory EPCs.

Detection of the Content of Serum Factors by Enzyme-Linked Immunosorbent Assay (ELISA)

5 mL venous blood of AIS patients was extracted and placed into non-anticoagulation tubes 1 d, 8 d, and 15 d after the intervention. ELISA was employed to detect the expression of vascular endothelial growth factor (VEGF), tumor necrosis factor-α (TNF-α), and interleukin-10 (IL)-10. The ELISA kit (RapidBio Systems, Inc., CA, USA) was employed to detect the expression of the above factors according to the kit instructions. A microplate reader (Bio-Rad Laboratories, Inc., CA, USA) was utilized to measure the absorbance of all specimens at 450 nm. Besides, ELISA was adopted to detect the changes of stromal cell-derived factor-1α (SDF-1α) in the two groups before and after treatment.

Statistical Analysis

SPSS 22.0 (IBM Corp., Armonk, NY, USA) was employed for the statistical analysis of research data. Measurement data were denoted by mean±standard deviation ($\bar{x}\pm s$) and enumeration data were expressed as percentages (%). The difference in measurement data conforming to normal distribution and homogeneity of variance between the two groups was analyzed by *t*-test. Data that did not conform to normal distribution or homogeneity of variance were analyzed by non-parameter test or exact probability method. Enumeration data were analyzed by the Chi-square test. In addition, the correlation between various factors and indicators was analyzed by Pearson straight-line correlation analysis. $p<0.05$ indicated that the difference revealed statistical significance.

Results

Analysis of the Segmentation of MRI Images of AIS Patients Based on a Lightweight CNN Model

The diffusion-weighted imaging (DWI) of MRI images of patients with acute stroke showed high signal, indicating cell swelling, increased bound water, limited diffusion, and acute infarction. After CNN algorithm processing, MRI image quality was significantly improved. After LT-RCNN model processing, MRI image method could locate the location of the lesion and accurately segment the contour. The segmentation results of the lesion contour (green) were highly coexisting with the results of manual delineation (red) (Figure 1). The segmentation accuracy and

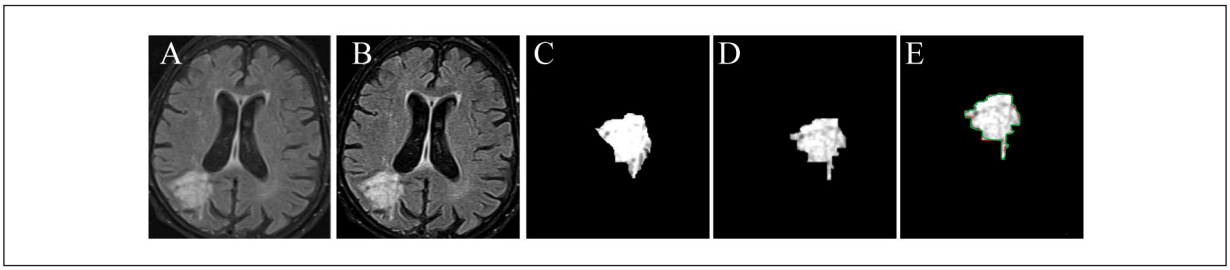

Figure 1. MRI images of patients with acute stroke. **A**, Initial MRI images of patients with acute stroke; (**B**) MRI images processed by CNN algorithm; (**C**) CNN algorithm segmentation of focal contour; (**D**) LT-RCNN model segmentation of focal contour; (**E**) comparison between LT-RCNN segmentation results and manual delineation results.

sensitivity of LT-RCNN model were (0.78±0.12) and (0.85±0.11), respectively, which were significantly higher than that of CNN model before optimization (0.61±0.14) and (0.72±0.13).

Comparison of Basic Data Between Two Groups

Gender ratio, average age, course of the disease, and the proportions of patients with different lesion sites in rehabilitation and conventional groups were compared and analyzed (Table I). No statistical differences were detected in the above basic data between the two groups (p>0.05).

Comparison of the Proportions of Patients with Different Histories Between the Two Groups

The proportions of patients with different histories in the two groups were statistically analyzed (Figure 2). The proportions of patients with histories of smoking, drinking, hypertension, diabetes, coronary disease, hyperlipidemia, and homocysteine in conventional and rehabilitation groups amounted to 20.83% (10 cases) *vs.* 24.00% (12 cases), 16.67% (8 cases) *vs.* 14.00 % (7 cases), 35.42% (17 cases) *vs.* 32.00% (16 cases), 12.50% (6 cases) *vs.* 16.00% (8 cases), 14.58% (7 cases) *vs.*. 12.00% (6 cases), 16.67% (8 cases) *vs.* 20.00% (10 cases), and 10.42% (5 cases) *vs.* 12.00% (6 cases), respectively. No statistical differences were detected in the proportions of patients with different histories between the two groups (p>0.05).

Evaluation of Rehabilitation Effects on Patients in Two Groups Treatment

FMA score was adopted to evaluate the rehabilitation effects of upper limbs among AIS patients after treatment (Figure 3). Before treatment, no statistical difference was revealed in FMA scores for patients in the conventional and rehabilitation groups (p>0.05). After treatment, FMA scores increased in both groups (p<0.05). FMA score for the rehabilitation group was superior to that for the conventional group (p<0.05).

MBI score was employed to evaluate AIS patients' daily living activities after treatment. In addition, MBI scores for the two groups before and after treatment were compared and analyzed (Figure 4). No statistical difference was revealed in MBI scores for the conventional and rehabilitation groups before treatment (p>0.05). After treatment, MBI scores for the conventional and rehabilitation groups amounted to 37.55±5.22 and 48.59±5.31, respectively. MBI scores for the conventional and rehabilitation groups after treatment

Table I. Comparison of basic data between two groups.

Factors	Conventional group (n=48)	Rehabilitation group (n=50)	χ^2/t-value	p-value
Gender			0.256	0.232
Male [cases (%)]	29 (60.42%)	28 (56.00%)		
Female [cases (%)]	19 (39.58%)	22 (44.00%)		
Age (years old)	66.82±8.64	65.57±9.53	0.456	0.387
Course of disease (hours)	16.31±1.56	17.05±1.43	0.513	0.401
Average duration of hospitalization (days)	13.72±1.38	14.11±1.58	1.287	0.186
Lesion sites			0.138	0.418
Left side	20 (41.67%)	21 (42.00%)		
Right side	28 (58.33%)	29 (58.00%)		

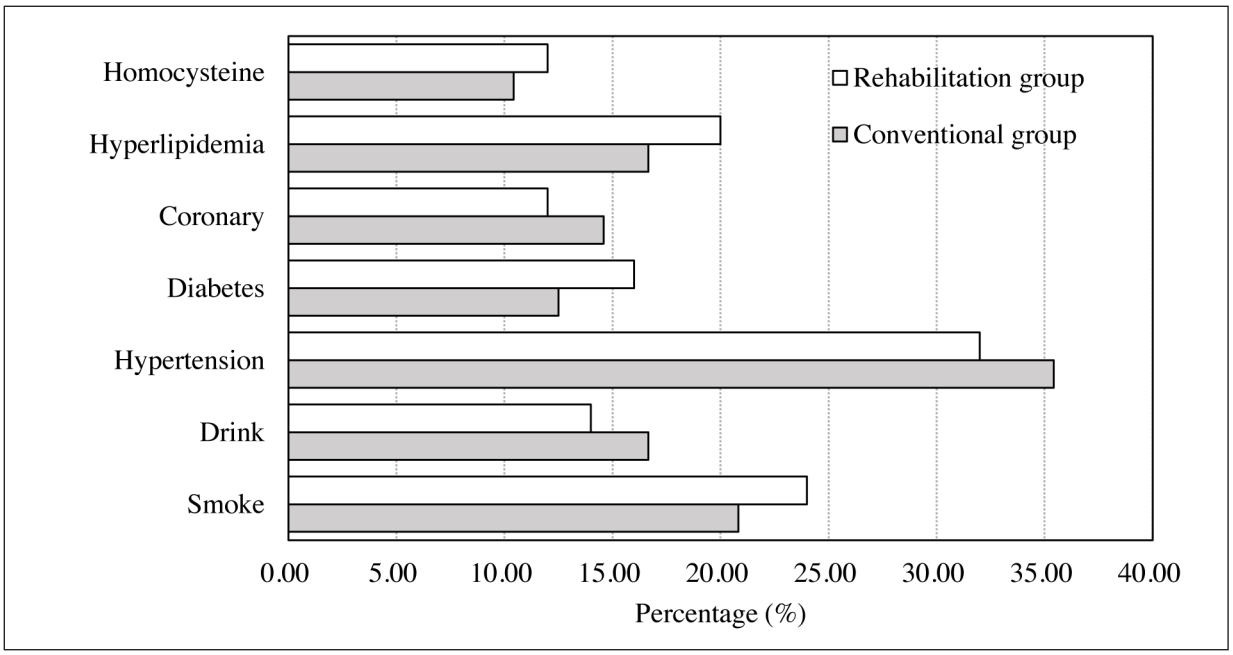

Figure 2. Comparison of the proportions of patients with different histories between the two groups.

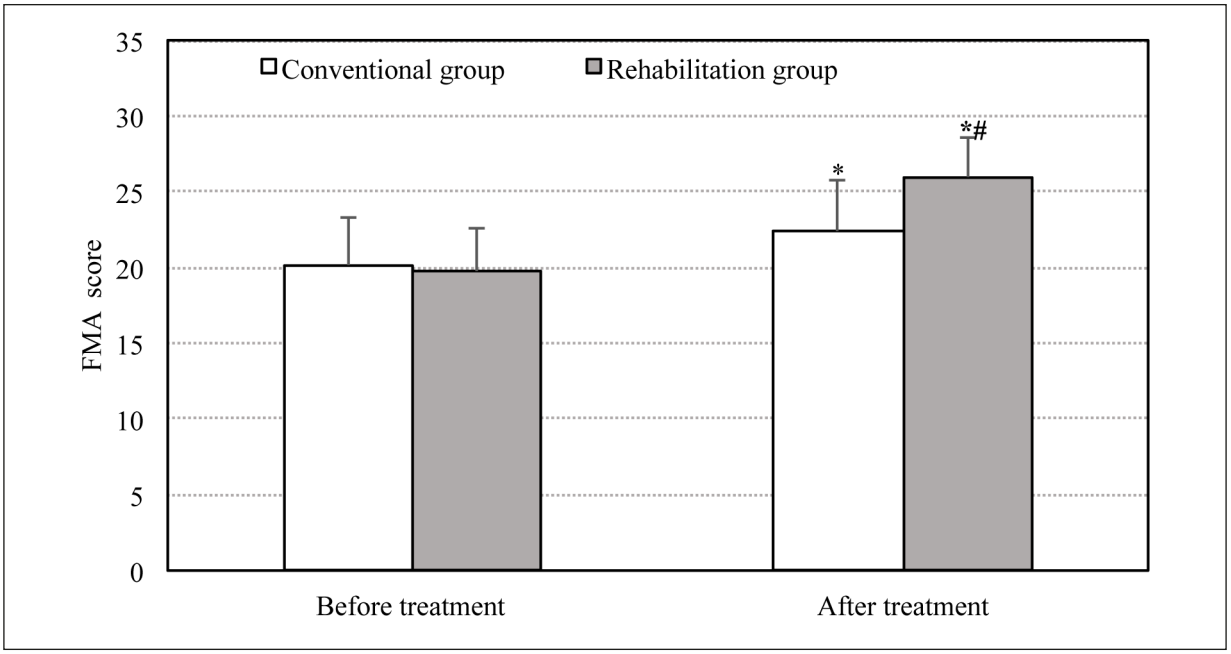

Figure 3. Comparison of Fugl-Meyer assessment (FMA) scores for the two groups after treatment. * Indicated that the comparison of MBI scores before and after treatment revealed a statistical difference ($p<0.05$). ** Indicated that the comparison of MBI scores before and after treatment revealed a significant difference ($p<0.01$). # Suggested that the comparison of the MBI score with the conventional group revealed a statistical difference ($p<0.05$).

were superior to those before treatment ($p<0.05$). The MBI score for the former one was inferior to that for the latter one ($p<0.05$).

NIHSS score was utilized to evaluate AIS patients' daily living activities after treatment. NIHSS scores for the two groups before and after treatment were compared and analyzed (Figure 5). No statistical difference was detected in NIHSS scores for the two groups before treatment ($p>0.05$). After treatment, NIHSS scores for

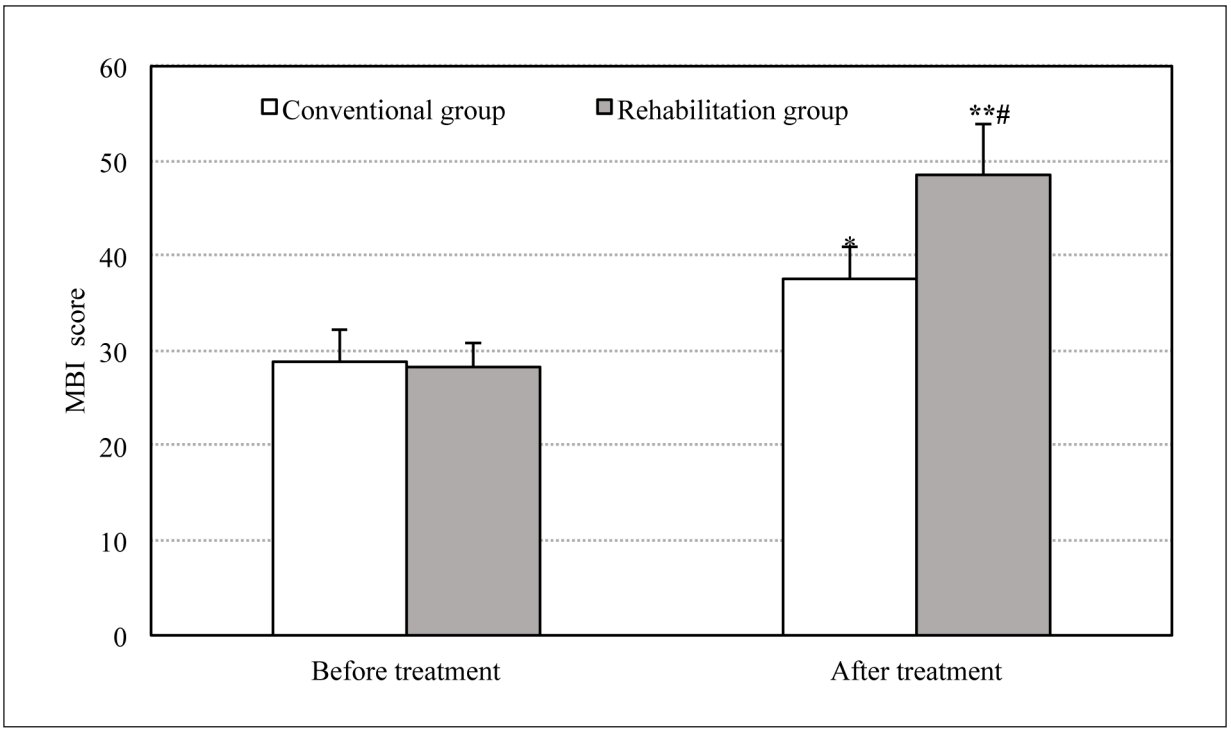

Figure 4. Comparison of MBI scores for the two groups after treatment. * Indicated that the comparison of MBI scores before and after treatment revealed a statistical difference (p<0.05). ** Indicated that the comparison of MBI scores before and after treatment revealed a significant difference (p<0.01). # Suggested that the comparison of the MBI score with the conventional group revealed a statistical difference (p<0.05).

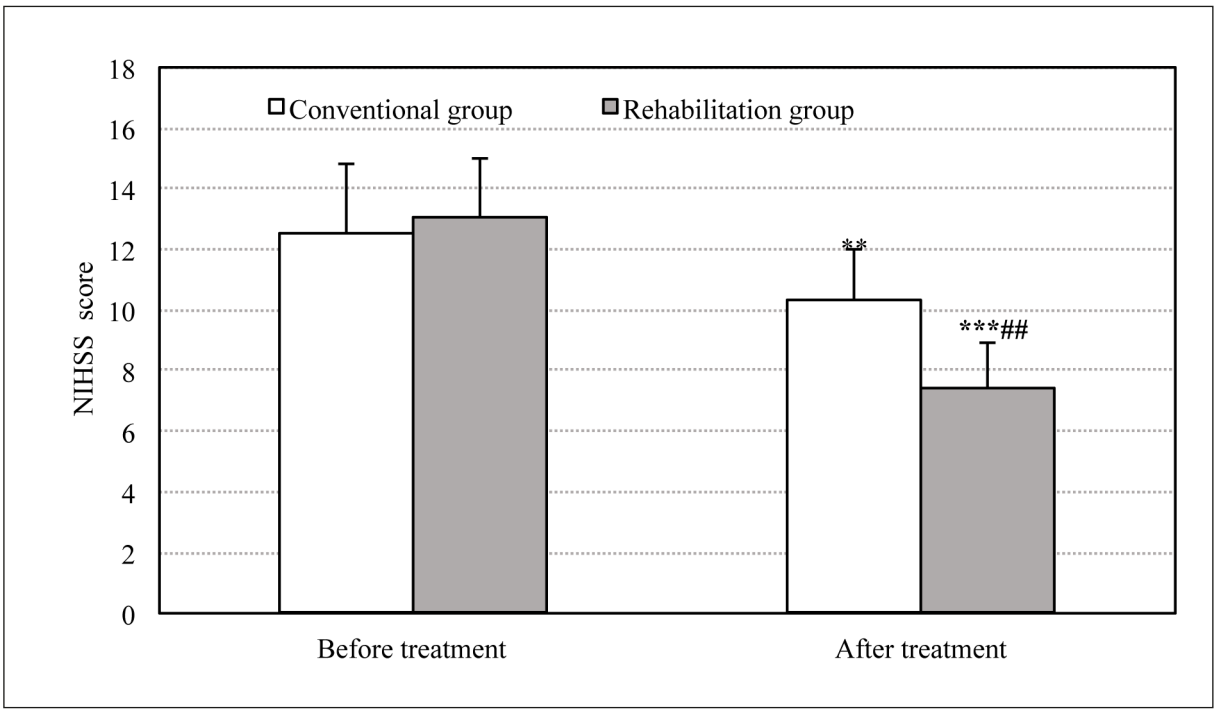

Figure 5. Comparison of NIHSS scores for the two groups after treatment. * Indicated that the comparison of MBI scores before and after treatment revealed a statistical difference (p<0.05). ** Indicated that the comparison of MBI scores before and after treatment revealed a significant difference (p<0.01). # Suggested that the comparison of the MBI score with the conventional group revealed a statistical difference (p<0.05).

the conventional and rehabilitation groups amounted to 10.37±1.62 and 7.42±1.54, respectively. After treatment, NIHSS scores for the conventional group apparently declined (p<0.01). An extremely significant difference was revealed in NIHSS scores for the rehabilitation group before and after treatment (p<0.001). The NIHSS score for the former was notably superior to that for the latter one (p<0.01).

Comparison of SS-QOL Scores for Two Groups

SS-QOL score was adopted to assess the change in quality of life of AIS patients before and after treatment (Figure 6). No statistical difference was revealed in SS-QOL scores for the conventional and rehabilitation groups before treatment (p>0.05). SS-QOL scores for the conventional and rehabilitation groups after treatment amounted to 161.47±5.61 and 177.72±18.04, respectively. After treatment, the SS-QOL scores of the two groups dramatically increased (p<0.05). SS-QOL score for the latter one was superior to that for the former one (p<0.05).

Comparison of the Number of CD34+, KDR+, and EPCs Cells between the Two Groups Before and After Treatment

The number of EPCs in the two groups 1 d, 8 d, and 15 d after treatment was compared (Figure 7). No statistical difference was detected in the number of EPCs between the two groups 1 d after treatment (p>0.05). The number of EPCs in the conventional and rehabilitation groups on the 8th day after treatment amounted to 75.50±6.24 cells/mL and 90.26±7.56 cells/mL, respectively. Apparently, the number of EPCs on the 8th day was notably superior to that on the 1st day in the conventional group (p<0.05). There was a remarkable difference in the number of EPCs on 1 d and 8 d in the rehabilitation group after treatment (p<0.01) and the number of EPCs on 8 d in the rehabilitation group was greater than that in the conventional group (p<0.05). After treatment, the number of EPCs on 15 d in the conventional and rehabilitation groups amounted to 93.31±8.16 cells/mL and 121.53±10.09 cells/mL, respectively. In the conventional group, the number of EPCs on 15 d apparently increased vs. that on 1 d (p<0.01). A noticeable difference was revealed in the number of EPCs on 15 d and 1 d in the rehabilitation group (p<0.001). The number of EPCs on the 15th day in the rehabilitation group was much greater than that in the conventional group after treatment (p<0.01).

The number of CD34+KDR+ cells in two groups 1 d, 8 d, and 15 d after treatment were compared (Figure 8). After treatment, no statistical difference was detected in the number of

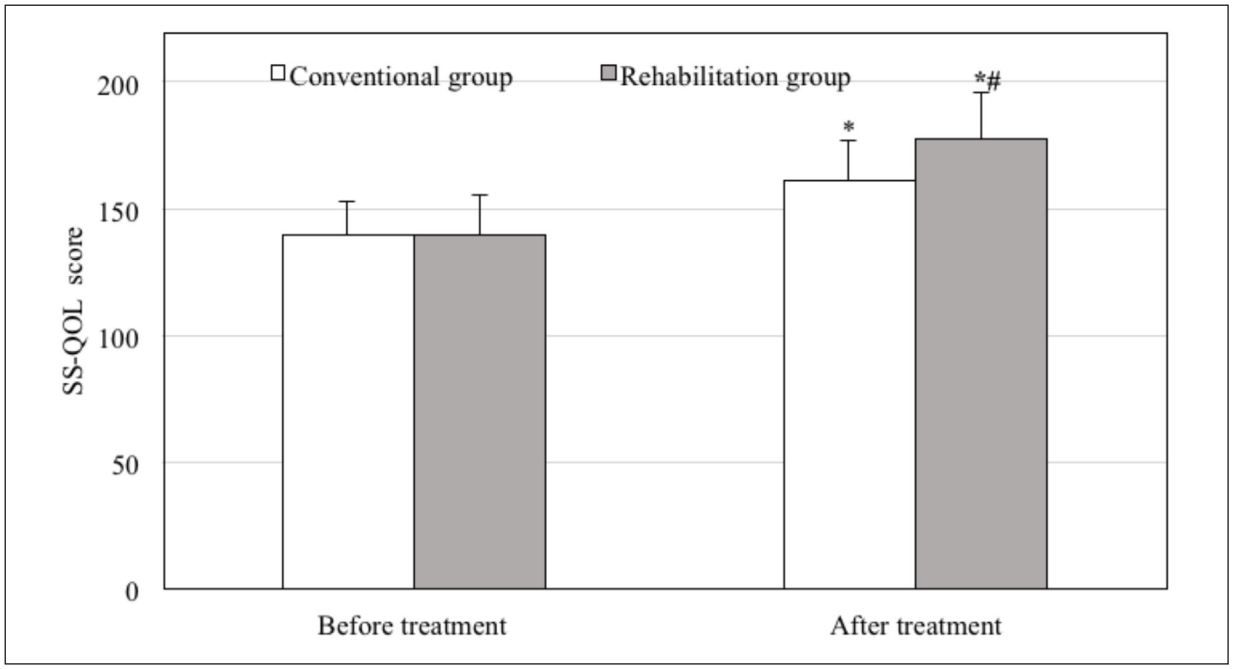

Figure 6. Comparison of stroke-specific quality of life (SS-QOL) scores for two groups after treatment. * Indicated that the comparison of MBI scores before and after treatment revealed a statistical difference (p<0.05). ** Indicated that the comparison of MBI scores before and after treatment revealed a significant difference (p<0.01). # Suggested that the comparison of the MBI score with the conventional group revealed a statistical difference (p<0.05).

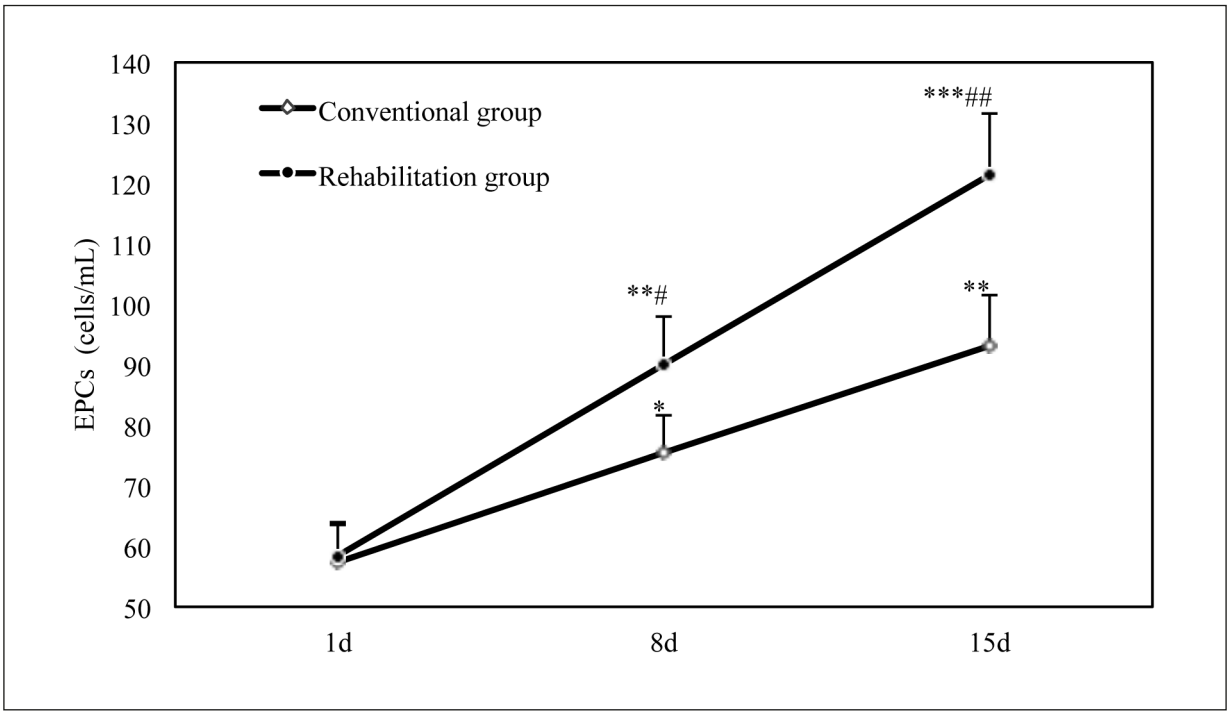

Figure 7. Comparison of the number of endothelial progenitor cells (EPCs) between two groups at different time periods after treatment. * Indicated that the comparison of MBI scores before and after treatment revealed a statistical difference (p<0.05). ** Indicated that the comparison of MBI scores before and after treatment revealed a significant difference (p<0.01). # Suggested that the comparison of the MBI score with the conventional group revealed a statistical difference (p<0.05).

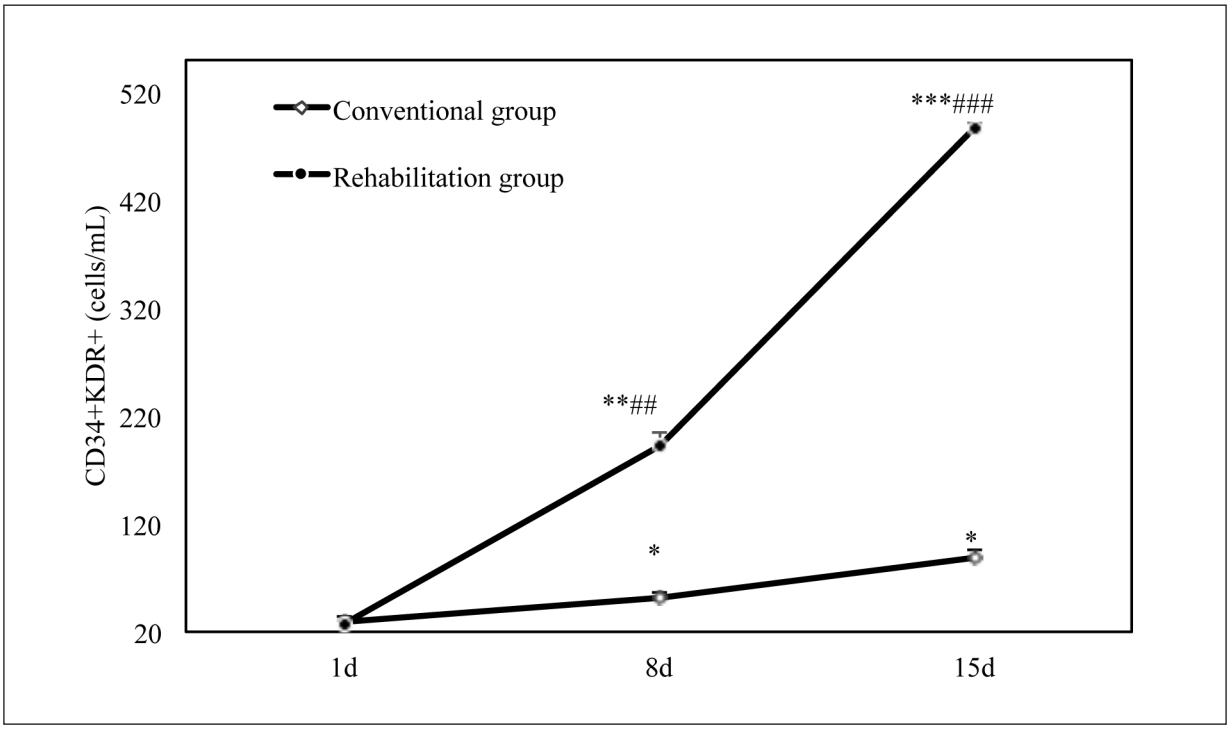

Figure 8. Comparison of the number of CD34+KDR+ cells between two groups at different time periods after treatment. * Indicated that the comparison of MBI scores before and after treatment revealed a statistical difference (p<0.05). ** Indicated that the comparison of MBI scores before and after treatment revealed a significant difference (p<0.01). # Suggested that the comparison of the MBI score with the conventional group revealed a statistical difference (p<0.05).

CD34+KDR+ cells between the two groups on 1 d (p>0.05). On the 8th day, the number of CD34+KDR+ cells in the conventional and rehabilitation groups amounted to 50.91±5.74 cells/mL and 192.38±12.43 cells/mL, respectively. The number of CD34+KDR+ cells in the conventional group on 8 d remarkably increased *vs.* that on 1 d after treatment. A significant difference was detected in the number of CD34+KDR+ cells in the rehabilitation group on 8 d and 1 d after treatment (p<0.01). The number of CD34+KDR+ cells in the latter group was notably greater than that in the former group 8 d after treatment (p<0.01). On the 15th day after treatment, the number of CD34+KDR+ cells in the conventional and rehabilitation groups amounted to 88.27±8.29 cells/mL and 487.54±3.72 cells/mL, respectively. The number of CD34+KDR+ cells in the conventional group on 15 d was apparently greater than that on 1 d (p<0.05). A conspicuous difference was revealed in the number of CD34+KDR+ cells in the rehabilitation group on 15 d and on 1 d (p<0.001). The number of CD34+KDR+ cells in the latter one was greater than that in the former one on 15 d with an extremely significant difference (p<0.001).

Comparison of the Contents of VEGF, TNF-α, and IL-10 Between the Two Groups

VEGF in two groups 1 d, 8 d, and 15 d after treatment were compared (Figure 9). No statistical difference was detected in VEGF contents between the two groups 1 d after treatment (p>0.05). On 8 d after treatment, VEGF in the conventional and rehabilitation groups amounted to 203.19±17.64 ng/L and 382.55±47.07 ng/L, respectively. VEGF in the conventional group on 8 d dramatically increased vs. that on 1 d (p<0.05). A remarkable difference was revealed in VEGF in the rehabilitation group on 8 d and 1 d (p<0.01). VEGF in the latter one was notably superior to that in the former one on 8 d (p<0.01). VEGF in the conventional and rehabilitation groups on 15 d amounted to 374.65±40.02 ng/L and 987.17±87.25 ng/L, respectively. VEGF in the conventional group on 15 d apparently increased vs. that on 1 d (p<0.05). A remarkable difference was detected in VEGF in this group on 15 d and 1 d (p<0.001). VEGF in the rehabilitation group was superior to that in the conventional group on 15 d with an extremely remarkable difference (p<0.001).

TNF-α in two groups 1 d, 8 d, and 15 d after treatment were compared (Figure 10). No statistical difference was revealed in TNF-α between the two groups on 1 d (p>0.05). TNF-α in the conventional and rehabilitation groups on 8 d amounted to 426.39±39.74 ng/L and 373.33±39.57 ng/L, respectively. In the former group, TNF-α on 8 d apparently declined *vs.* that on 1 d (p<0.05). In the latter group, a remarkable difference was revealed in TNF-α on 8 d and 1 d (p<0.01). TNF-α in the latter one was apparently inferior to that in the former one on 8 d (p<0.01). TNF-α in the conventional and rehabilitation groups on 15 d amounted to 374.76±35.52 ng/L and 158.50±16.18 ng/L, respectively. TNF-α on 15 d dramatically declined *vs.* that on 1 d in the conventional group (p<0.01). A significant difference was detected in TNF-α on 15 d and 1 d in another group (p<0.001). TNF-α in the rehabilitation group was inferior to that in another group on 15 d (p<0.001).

IL-10 in two groups 1 d, 8 d, and 15 d after treatment were compared (Figure 11). No statistical difference was revealed in IL-10 between the two groups on 1 d (p>0.05). IL-10 in the conventional group on 8 d apparently increased *vs.* that on 1 d (p<0.05). An important difference was detected in IL-10 in the rehabilitation group on 8 d and 1 d (p<0.01). IL-10 in the latter one was dramatically superior to that in the former one on 8 d (p<0.01). In the conventional group, IL-10 on 15 d notably improved vs. that on 1 d (p<0.01). A significant difference was detected in IL-10 in the rehabilitation group on 15 d and 1 d (p<0.001). IL-10 in the latter one was superior to that in the former one on 15 d (p<0.001).

Comparison of SDF-1α Between two Groups Before and After Treatment

SDF-1α in two groups on 1 d, 8 d, and 15 d after treatment were compared (Figure 12). No statistical difference was revealed in SDF-1α between the two groups on 1d (p>0.05). SDF-1α on 8 d apparently improved vs. that on 1 d in the conventional group (p<0.05). A significant difference was detected in SDF-1α on 8 d and 1 d in the rehabilitation group (p<0.01). SDF-1α in the latter one was apparently superior to that in the former one on 8 d (p<0.01). SDF-1α on 15 d was much superior to that on 1 d in the conventional group (p<0.01). A remarkable difference was detected in SDF-1α on 15 d and 1 d in the rehabilitation group (p<0.001). SDF-1α in the latter one was superior to that in the former one on 15 d (p<0.001).

Correlation Analysis

The correlation between CD34+KDR+ and VEGF among AIS patients was analyzed (Figure 13). The number of CD34+KDR+ cells was positively correlated with VEGF content (r=0.7002, p=0.004).

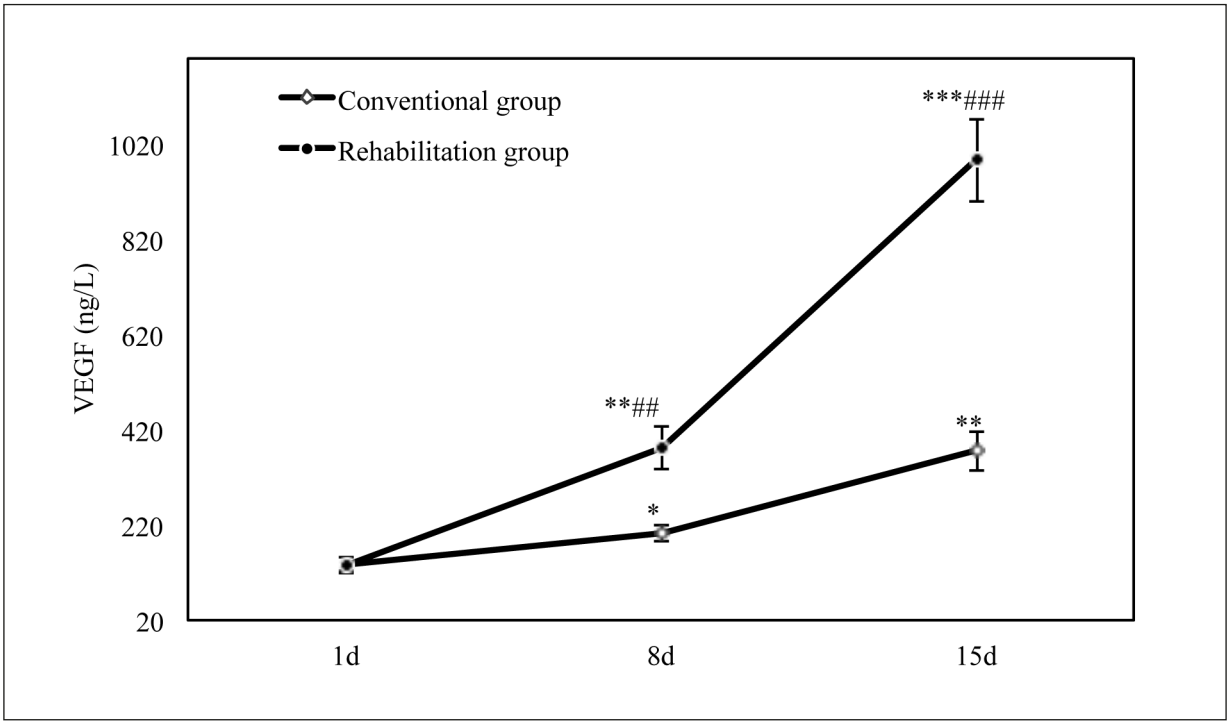

Figure 9. Comparison of vascular endothelial growth factor (VEGF) contents between two groups. * Indicated that the comparison of MBI scores before and after treatment revealed a statistical difference (p<0.05). ** Indicated that the comparison of MBI scores before and after treatment revealed a significant difference (p<0.01). # Suggested that the comparison of the MBI score with the conventional group revealed a statistical difference (p<0.05).

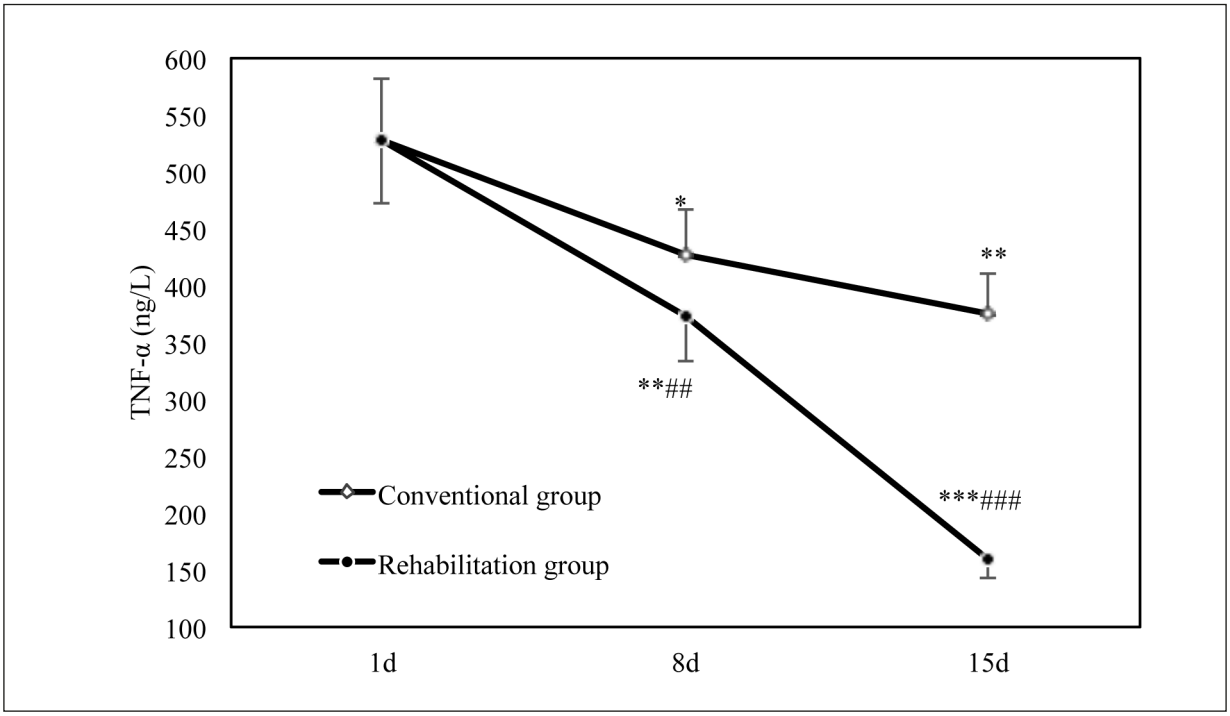

Figure 10. Comparison of tumor necrosis factor-α (TNF-α) between two groups. * Indicated that the comparison of MBI scores before and after treatment revealed a statistical difference (p<0.05). ** Indicated that the comparison of MBI scores before and after treatment revealed a significant difference (p<0.01). # Suggested that the comparison with the MBI score with the conventional group revealed a statistical difference (p<0.05).

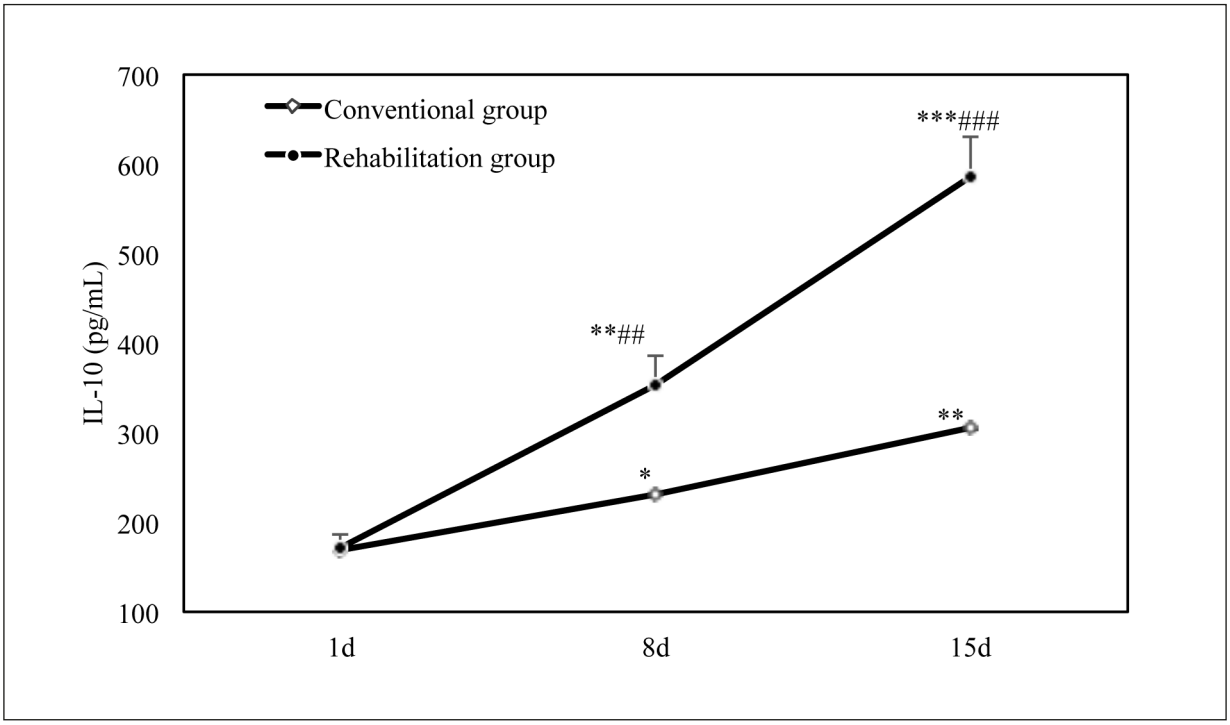

Figure 11. Comparison of interleukin-10 (IL-10) between two groups. * Indicated that the comparison of MBI scores before and after treatment revealed a statistical difference ($p<0.05$). ** Indicated that the comparison of MBI scores before and after treatment revealed a significant difference ($p<0.01$). # Suggested that the comparison with the MBI score with the conventional group revealed a statistical difference ($p<0.05$).

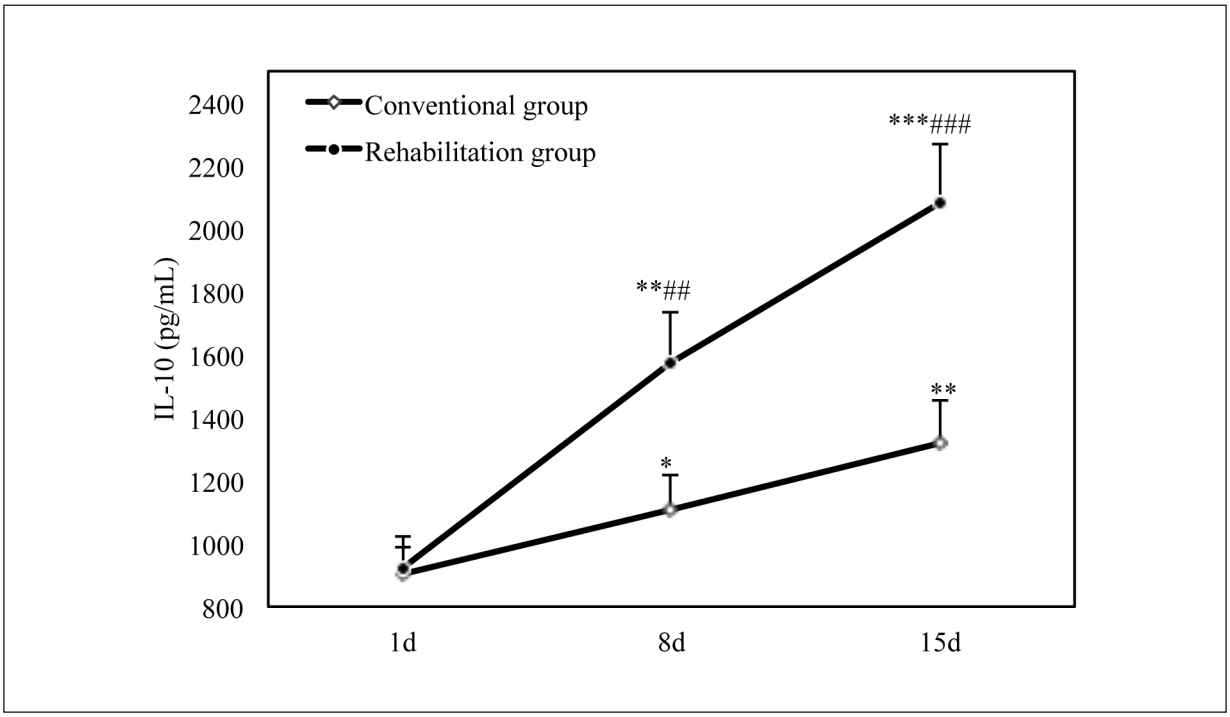

Figure 12. Comparison of stromal cell-derived factor-1α (SDF-1α) between two groups. * Indicated that the comparison of MBI scores before and after treatment revealed a statistical difference ($p<0.05$). ** Indicated that the comparison of MBI scores before and after treatment revealed a significant difference ($p<0.01$). # Suggested that the comparison with the MBI score with the conventional group revealed a statistical difference ($p<0.05$).

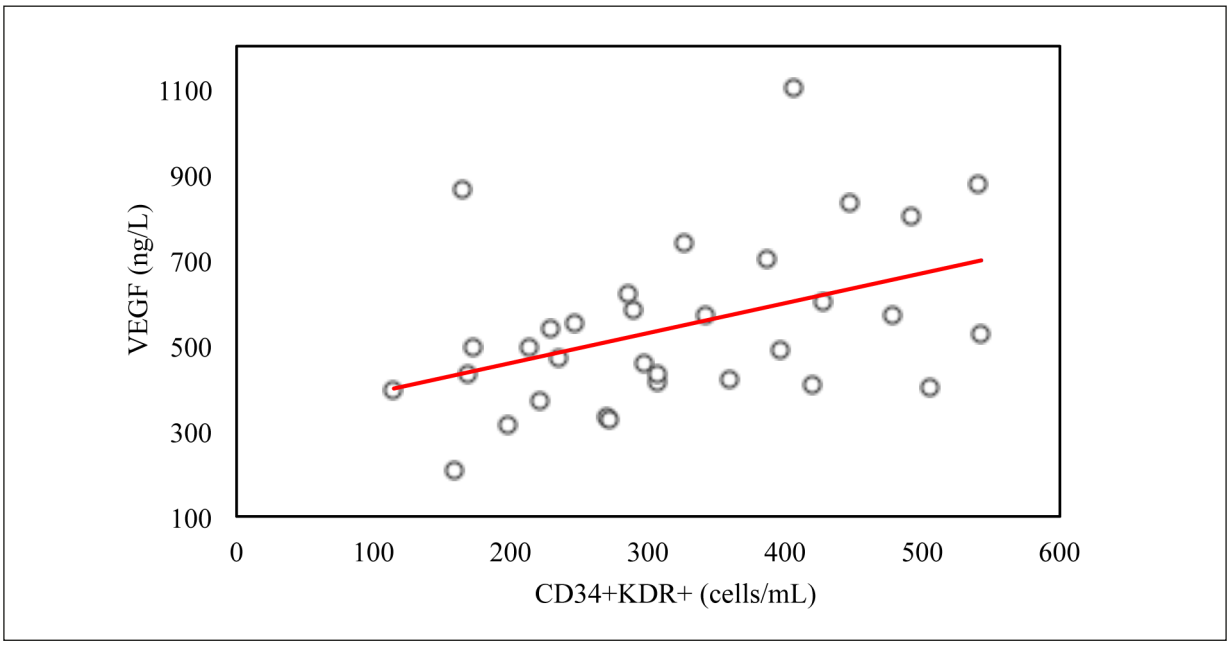

Figure 13. Analysis of the correlation between CD34+KDR+ and VEGF.

The correlation between CD34+KDR+ and IL-10 among AIS patients was analyzed (Figure 14). The number of CD34+KDR+ cells was positively correlated with IL-10 (r=0.5231, p=0.006). Finally, the correlation between CD34+KDR+ and TNF-α was analyzed in Figure 15.

Discussion

AIS is the commonest cerebrovascular disease that is usually caused by blood circulatory disorders in local brain tissues or ischemia- and hypoxia-induced brain tissue softening[27]. The incidence of AIS among elderly people is the highest[28]. According to relevant statistical results[29], about 80% of people suffer from different levels of sequelae among all AIS survivors, especially limb and neurological dysfunctions[30]. Early rehabilitation training refers to the rehabilitation scheme formulated for the diagnosis of disease at the initial stage of treatment[31]. The current research findings reveal that cell necrosis is irreversible after the occurrence of AIS. However, some of the peripheral tissue functions are restored[32]. Some scholars pointed out that early rehabilitation training for AIS patients could promote the generation of new synapses in penumbra regions, which were conducive to the rehabilitation of neurological and limb motor functions[33]. At present, no consensus has been reached on the intervention time of rehabilitation training for patients with stroke. In addition, it was pointed out that rehabilitation training should be performed after the disease became stable[34]. Han et al[35] believed that early rehabilitation training was more conducive to the rehabilitation of limb motor function of patients with stroke. Based on radical therapy, all included AIS patients underwent early rehabilitation training. It was revealed that the NIHSS score for the rehabilitation group was notably inferior to that for the conventional group (p<0.01). The above research findings demonstrated that early rehabilitation training could effectively promote the rehabilitation of upper limb and neurological functions, enhance the activity of daily living, and improve the postoperative quality of life of AIS patients, which was similar to the research outcome obtained by Nemchek et al[36].

CD34 is a cell adhesion molecule that can be expressed on hemopoietic stem cells. KDR is associated with the differentiation of early endothelial cells. CD34+KDR+ is the main circulatory EPCs in blood[37]. Hence, the content of peripheral circulatory EPCs of AIS patients was detected based on CD34+KDR+ in the research. It was suggested that the number of EPCs in the rehabilitation group was much greater than that in the conventional group on 15 d after treatment (p<0.01). After different treatment methods were adopted, the number of EPCs apparently increased, especially among patients undergoing early

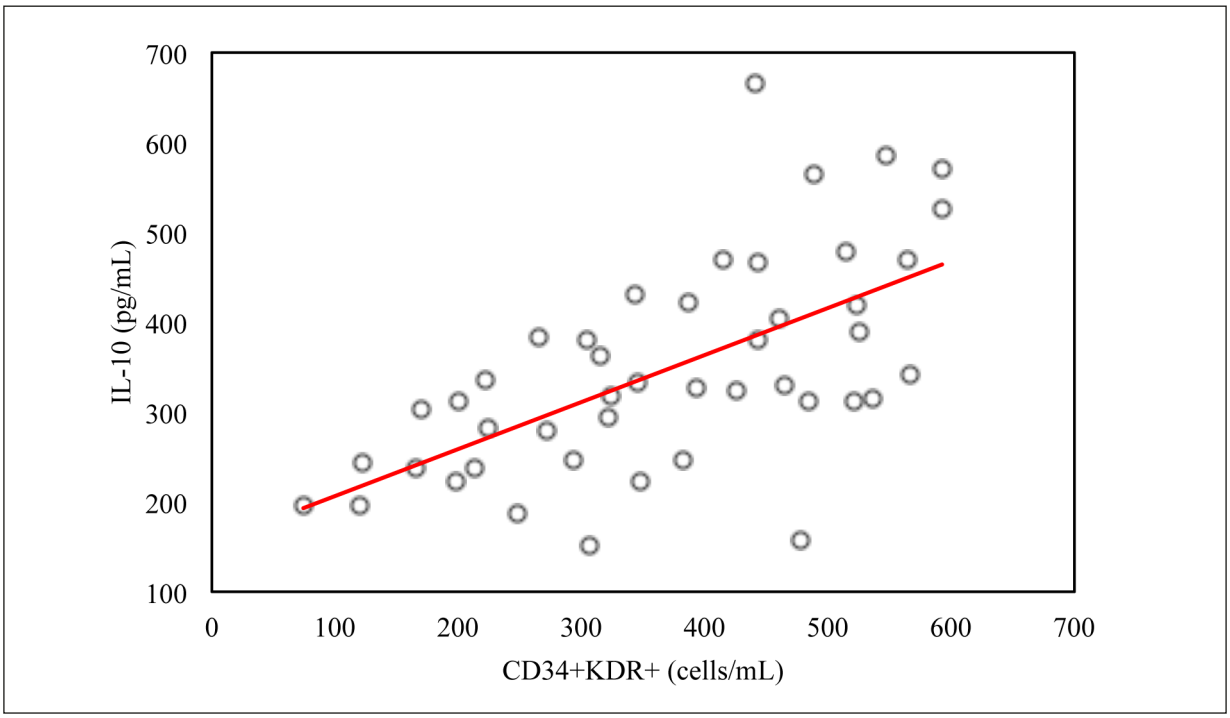

Figure 14. Analysis of the correlation between CD34+KDR+ and IL-10.

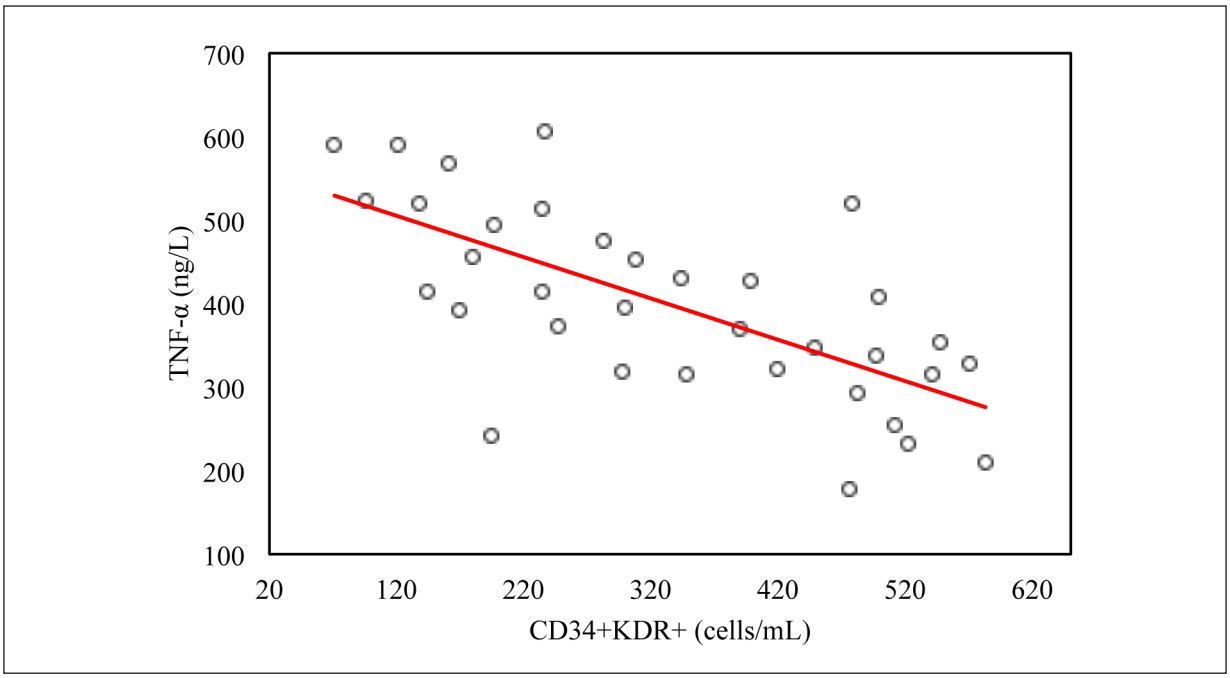

Figure 15. Analysis of the correlation between CD34+KDR+ and TNF-α.

rehabilitation training. The findings indicated that EPCs could be mobilized from bone marrow because of exercise training, Yue et al[38] showed that local ischemia induced the mobilization of EPCs and promoted the change in the expression of matrix metalloproteinase (MMP). At present, some research findings reveal that rehabilitation training can promote the change of MMP-9. It was speculated that the change was related to EPCs mobilization-induced neoangiogenesis[39]. In

addition, it was pointed out that rehabilitation training could activate endothelial nitric oxide synthase to promote the rise of MMP-9 and MMP-2 and affect the expression of SDF-1α. Consequently, EPCs were mobilized into peripheral blood[40]. The research result of SDF-1α in the rehabilitation group was superior to that in the conventional group on 15 d (p<0.001), suggesting that rehabilitation training could increase SDF-1a. Liu et al[41] reckoned that EPCs homed in tissues under the action of SDF-1α after entering peripheral blood.

VEGF is an angiogenic factor that plays a vital role in the proliferation of endothelial cells and angiogenesis. Yang et al[42] revealed that EPCs homing to ischemic tissues could secrete VEGF. According to the research findings, VEGF in the rehabilitation group was superior to that in the conventional group on 15 d (p<0.001), demonstrating that early rehabilitation training could effectively increase VEGF in peripheral blood, which might be achieved by promoting EPCs mobilization. What's more, it was found that EPCs were positively correlated with VEGF, which revealed that the rise of EPCs in peripheral blood among AIS patients might be associated with the increase of VEGF[43]. TNF-α is a proinflammatory cytokine that can stimulate the secretion of acute phase proteins and the expression of other inflammatory cytokines and cell adhesion factors. It was suggested that TNF-α was related to the severity of early stroke and neurological injury. IL-10 is an anti-inflammatory cytokine that can inhibit the expression of TNF-α and inflammatory cytokines. It was indicated in some research that the injection of IL-10 into stroke model animals could effectively protect their cranial nerves. According to the research outcomes, TNF-α in the rehabilitation group was inferior to that in the conventional group on 15 d (p<0.001), while IL-10 in the former one was superior to that in the latter one on 15 d (p<0.001). The results suggested that early rehabilitation training could effectively promote IL-10 expression and inhibit TNF-α expression, which might be associated with EPCs mobilization. Loiola et al[44] pointed out that rehabilitation training could increase IL-10 in ischemic brain tissues, which was similar to our research outcome.

Conclusions

In the research, CNN algorithm was optimized to establish LT-RCNN learning model and apply it in processing the diagnostic MRI images of AIS patients. It was found that DWI hyperintensity in MRI images of AIS patients and LT-RCNN model could localize the position of lesions and accurately segment the contours of lesions. The therapeutic effects of early rehabilitation training on AIS patients were analyzed and its influences and action mechanisms on circulatory EPCs mobilization among AIS patients were investigated. It was revealed that early rehabilitation training could promote circulatory EPCs mobilization. The possible mechanism was based on the promotion of VEGF and IL-10 expression and the inhibition of SDF-1α among AIS patients. Nevertheless, there are still some shortcomings in the research. The influences of early rehabilitation training on AIS patients and its possible mechanisms were only preliminarily discussed. In follow-up research, the research findings need to be further verified based on animal experiments. In conclusion, the research provided a referable basis for the diagnosis, treatment, and prognosis of AIS patients.

Ethics Approval

The experimental procedures had been approved by Hospital Ethics Committee of People's Hospital of Yanshan County, Ethics approval acceptance number No. 204106055. All included research objects had signed informed consent forms.

Informed Consent

The subjects included in this study were all aware of the study and had signed informed consent.

Authors' Contributions

All authors of this study participated in the experimental design, sample collection, data statistics, and analysis, and participated in writing, proofreading, text editing, language revision, chart drawing, and final review of the paper.

Data Availability

Data for this work are publicly available in the text and raw data are available from the authors.

ORCID ID

Lei Sun: 0009-0007-3568-1669

Conflict of Interest

The authors declare that they have no conflicts of interest.

Funding

This work was supported by the key research and development plan guidance project of Cangzhou City, Hebei Province, the

intervention effect and mechanism of early rehabilitation on patients with acute ischemic stroke (Project No. 204106055).

References

1) Hurford R, Sekhar A, Hughes TAT, Muir KW. Diagnosis and management of acute ischaemic stroke. Pract Neurol 2020; 20: 304-316.
2) Tater P, Pandey S. Post-stroke Movement Disorders: Clinical Spectrum, Pathogenesis, and Management. Neurol India 2021; 69: 272-283.
3) Barthels D, Das H. Current advances in ischemic stroke research and therapies. Biochim Biophys Acta Mol Basis Dis 2020; 1866: 165260.
4) Taner Bulut H, Altun Y, Arik A, Oktay C, Çorapli M. Use of multiparametric magnetic resonance imaging as a screening tool for the determination of acute ischemic stroke duration. Eur Rev Med Pharmacol Sci 2022; 26: 846-852.
5) Lv Z, Qiao L, Li J, Song H. Deep-learning-enabled security issues in the internet of things. IEEE Internet of Things Journal 2020; 812, 9531-9538.
6) Saha S, Pagnozzi A, Bourgeat P. Predicting motor outcome in preterm infants from very early brain diffusion MRI using a deep learning convolutional neural network (CNN) model. Neuroimage 2020; 215: 116807.
7) Mendelson SJ, Prabhakaran S. Diagnosis and Management of Transient Ischemic Attack and Acute Ischemic Stroke: A Review. JAMA 2021; 325: 1088-1098.
8) Zi W, Qiu Z, Li F, Effect of Endovascular Treatment Alone vs Intravenous Alteplase Plus Endovascular Treatment on Functional Independence in Patients With Acute Ischemic Stroke: The DEVT Randomized Clinical Trial. JAMA 2021; 325: 234-243.
9) Lin RC, Chiang SL, Heitkemper MM, Weng SM, Lin CF, Yang FC, Lin CH. Effectiveness of Early Rehabilitation Combined With Virtual Reality Training on Muscle Strength, Mood State, and Functional Status in Patients With Acute Stroke: A Randomized Controlled Trial. Worldviews Evid Based Nurs 2020; 17: 158-167.
10) Wang J, Zhang Y, Chen Y, Li M, Yang H, Chen J, Tang Q, Jin J. Effectiveness of Rehabilitation Nursing versus Usual Therapist-Led Treatment in Patients with Acute Ischemic Stroke: A Randomized Non-Inferiority Trial. Clin Interv Aging 2021; 16: 1173-1184.
11) Suzuki K, Matsumaru Y, Takeuchi M. Effect of Mechanical Thrombectomy Without vs With Intravenous Thrombolysis on Functional Outcome Among Patients With Acute Ischemic Stroke: The SKIP Randomized Clinical Trial. JAMA 2021; 325: 244-253.
12) Yang L, Han B, Zhang Z. Extracellular Vesicle-Mediated Delivery of Circular RNA SCMH1 Promotes Functional Recovery in Rodent and Nonhuman Primate Ischemic Stroke Models. Circulation 2020; 142: 556-574.
13) Hatakeyama M, Ninomiya I, Kanazawa M. Angiogenesis and neuronal remodeling after ischemic stroke. Neural Regen Res 2020; 15: 16-19.
14) Camps-Renom P, Jiménez-Xarrié E, Soler M. Endothelial Progenitor Cells Count after Acute Ischemic Stroke Predicts Functional Outcome in Patients with Carotid Atherosclerosis. J Stroke Cerebrovasc Dis 2021; 30: 106144.
15) Li J, Ma Y, Miao XH, Guo JD, Li DW. Neovascularization and tissue regeneration by endothelial progenitor cells in ischemic stroke. Neurol Sci 202; 42: 3585-3593.
16) Guo W, Liu Z, Lu Q. Non-Linear Association Between Serum Alkaline Phosphatase and 3-Month Outcomes in Patients With Acute Stroke: Results From the Xi'an Stroke Registry Study of China. Front Neurol 2022; 13: 859258.
17) Rakkar K, Othman O, Sprigg N, Bath P, Bayraktutan U. Endothelial progenitor cells, potential biomarkers for diagnosis and prognosis of ischemic stroke: protocol for an observational case-control study. Neural Regen Res 2020; 15: 1300-1307.
18) Zhao W, Zhang J, Liao J, Li X. Evaluation of circulating endothelial progenitor cells and the severity of transient ischemic attack. J Clin Neurosci 2022; 99: 123-129.
19) Sharma P, Ninomiya T, Omodaka K, Takahashi N, Miya T, Himori N, Okatani T, Nakazawa T. A lightweight deep learning model for automatic segmentation and analysis of ophthalmic images. Sci Rep 2022; 12: 8508.
20) Du X, Liu M, Sun Y. Segmentation, Detection, and Tracking of Stem Cell Image by Digital Twins and Lightweight Deep Learning. Comput Intell Neurosci 2022; 2022: 6003293.
21) Özbek M, Akıl MA, Demir M, Arık B, Demir F, Akıl E. Prognostic importance of nutritional assessment in patients with acute ischemic stroke undergoing endovascular thrombectomy. Eur Rev Med Pharmacol Sci 2023; 27: 960-968.
22) Zhou X, Li Y, Liang W. CNN-RNN Based Intelligent Recommendation for Online Medical Pre-Diagnosis Support. IEEE/ACM Trans Comput Biol Bioinform 2021; 18: 912-921.
23) Cheng C, Fan W, Liu C, Liu Y, Liu X. Reminiscence therapy-based care program relieves post-stroke cognitive impairment, anxiety, and depression in acute ischemic stroke patients: a randomized, controlled study. Ir J Med Sci 2021; 190: 345-355.
24) Sandberg K, Kleist M, Enthoven P, Wijkman M. Hemodynamic responses to In-Bed Cycle Exercise in the acute phase after moderate to severe stroke: A randomized controlled trial. J Clin Hypertens (Greenwich) 2021; 23: 1077-1084.
25) Shang X, Meng X, Xiao X, Xie Z, Yuan X. Grip training improves handgrip strength, cognition, and brain white matter in minor acute ischemic

stroke patients. Clin Neurol Neurosurg 2021; 209: 106886.

26) Yazdani M, Chitsaz A, Zolaktaf V. Can Early Neuromuscular Rehabilitation Protocol Improve Disability after a Hemiparetic Stroke? A Pilot Study. Brain Sci 2022; 12: 816.

27) Wu WX, Zhou CY, Wang ZW. Effect of Early and Intensive Rehabilitation after Ischemic Stroke on Functional Recovery of the Lower Limbs: A Pilot, Randomized Trial. J Stroke Cerebrovasc Dis 2020; 29: 104649.

28) Chen H, Shi M, Geng W, Jiang L, Yin X, Chen YC. A preliminary study of cortical morphology changes in acute brainstem ischemic stroke patients. Medicine (Baltimore) 2021; 100: e24262.

29) Ghozy S, Kacimi SEO, Azzam AY, Farahat RA, Abdelaal A, Kallmes KM, Adusumilli G, Heit JJ, Kadirvel R, Kallmes DF. Successful mechanical thrombectomy in acute ischemic stroke: revascularization grade and functional independence. J Neurointerv Surg 2022; 14: 779-782.

30) Ouyang F, Jiang Z, Chen X. Is Cerebral Amyloid-β Deposition Related to Post-stroke Cognitive Impairment. Transl Stroke Res 2021; 12: 946-957.

31) Best JG, Ambler G, Wilson D. Development of imaging-based risk scores for prediction of intracranial haemorrhage and ischaemic stroke in patients taking antithrombotic therapy after ischaemic stroke or transient ischaemic attack: a pooled analysis of individual patient data from cohort studies. Lancet Neurol 2021; 20: 294-303.

32) Thomas RJ, Beatty AL, Beckie TM. Home-Based Cardiac Rehabilitation: A Scientific Statement From the American Association of Cardiovascular and Pulmonary Rehabilitation, the American Heart Association, and the American College of Cardiology. J Am Coll Cardiol 2019; 74: 133-153.

33) Correia PN, Meyer IA, Eskandari A, Amiguet M, Hirt L, Michel P. Preconditioning by Preceding Ischemic Cerebrovascular Events. J Am Heart Assoc 2021; 10: e020129.

34) Wolf TJ, Doherty M, Boone A. Cognitive oriented strategy training augmented rehabilitation (COSTAR) for ischemic stroke: a pilot exploratory randomized controlled study. Disabil Rehabil 2021; 43: 201-210.

35) Han Z, Zhao W, Lee H. Remote Ischemic Conditioning with Exercise (RICE)-Rehabilitative Strategy in Patients With Acute Ischemic Stroke: Rationale, Design, and Protocol for a Randomized Controlled Study. Front Neurol 2021; 12: 654669.

36) Nemchek V, Haan EM, Kerr AL. Intermittent Skill Training Results in Moderate Improvement in Functional Outcome in a Mouse Model of Ischemic Stroke. Neurorehabil Neural Repair 2021; 35: 79-87.

37) Custodia A, Ouro A, Sargento-Freitas J. Unraveling the potential of endothelial progenitor cells as a treatment following ischemic stroke. Front Neurol 2022; 13: 940682.

38) Yue Y, Wang C, Benedict Cl. Interleukin-10 Deficiency Alters Endothelial Progenitor Cell-Derived Exosome Reparative Effect on Myocardial Repair via Integrin-Linked Kinase Enrichment. Circ Res 2020; 126: 315-329.

39) Kukumberg M, Zaw AM, Wong DHC. Characterization and Functional Assessment of Endothelial Progenitor Cells in Ischemic Stroke Patients. Stem Cell Rev Rep 2021; 17: 952-967.

40) Alwjwaj M, Kadir RRA, Bayraktutan U. The secretome of endothelial progenitor cells: a potential therapeutic strategy for ischemic stroke. Neural Regen Res 2021; 16: 1483-1489.

41) Liu R, Zheng Y, Han T, Lan J, He L, Shi J. Angiogenic Actions of Paeoniflorin on Endothelial Progenitor Cells and in Ischemic Stroke Rat Model. Am J Chin Med 2021; 49: 863-881.

42) Yang Y, Yang LY, Salayandia VM, Thompson JF, Torbey M, Yang Y. Treatment with Atorvastatin During Vascular Remodeling Promotes Pericyte-Mediated Blood-Brain Barrier Maturation Following Ischemic Stroke. Transl Stroke Res 2021; 12: 905-922.

43) Zhou J, Li H, Xun L, Wang L, Zhao Q. Hyperlipidemia attenuates the mobilization of endothelial progenitor cells induced by acute myocardial ischemia via VEGF/eNOS/NO/MMP-9 pathway. Aging (Albany NY) 2022; 14: 7877-7889.

44) Loiola RA, García-Gabilondo M, Grayston A. Secretome of endothelial progenitor cells from stroke patients promotes endothelial barrier tightness and protects against hypoxia-induced vascular leakage. Stem Cell Res Ther 2021; 12: 552.